



A PGC1- α -dependent Myokine that Drives Brown-fat-like Development of White Fat and Thermogenesis

Citation

Boström, Pontus, Jun Wu, Mark P. Jedrychowski, Anisha Korde, Li Ye, James C. Lo, Kyle A. Rasbach, et al. 2012. A PGC1- α -dependent myokine that drives brown-fat-like development of white fat and thermogenesis. *Nature* 481(7382): 463-468.

Published Version

doi:10.1038/nature10777

Permanent link

<http://nrs.harvard.edu/urn-3:HUL.InstRepos:10579551>

Terms of Use

This article was downloaded from Harvard University's DASH repository, and is made available under the terms and conditions applicable to Other Posted Material, as set forth at <http://nrs.harvard.edu/urn-3:HUL.InstRepos:dash.current.terms-of-use#LAA>

Share Your Story

The Harvard community has made this article openly available.
Please share how this access benefits you. [Submit a story](#).

[Accessibility](#)

Published in final edited form as:

Nature. ; 481(7382): 463–468. doi:10.1038/nature10777.

A PGC1 α -dependent myokine that drives browning of white fat and thermogenesis

Pontus Boström¹, Jun Wu¹, Mark P. Jedrychowski², Anisha Korde¹, Li Ye¹, James C. Lo¹, Kyle A. Rasbach¹, Elisabeth Almer Boström³, Jang Hyun Choi¹, Jonathan Z. Long¹, Shingo Kajimura⁴, Maria Cristina Zingaretti⁵, Birgitte F. Vind⁶, Hua Tu⁷, Saverio Cinti⁵, Kurt Højlund⁶, Steven P. Gygi², and Bruce M. Spiegelman^{1,*}

¹Dana-Farber Cancer Institute and Harvard Medical School, 3 Blackfan Circle, CLS Building, floor 11, Boston, MA, 02115, USA

²Department of Cell Biology, Harvard Medical School, Boston, MA, 02115, USA

³Renal Division, Brigham and Women's Hospital, Harvard Medical School

⁴UCSF Diabetes Center and Department of Cell and Tissue Biology, University of California, San Francisco

⁵Department of Experimental and Clinical Medicine, Università Politecnica delle Marche, Electron Microscopy Unit-Azienda Ospedali Riuniti, Ancona 60020, Italy

⁶Diabetes Research Center, Department of Endocrinology, Odense University Hospital, Denmark

⁷LakePharma, Inc. 530 Harbor Blvd, Belmont CA 94002

Abstract

Exercise benefits a variety of organ systems in mammals, and some of the best-recognized effects of exercise on muscle are mediated by the transcriptional coactivator PGC1 α . Here we show that PGC1 α expression in muscle stimulates an increase in expression of Fndc5, a membrane protein that is cleaved and secreted as a new hormone, irisin. Irisin acts on white adipose cells in culture and *in vivo* to stimulate UCP1 expression and a broad program of brown fat-like development. Irisin is induced with exercise in mice and humans, and mildly increased irisin levels in blood cause an increase in energy expenditure in mice with no changes in movement or food intake. This results in improvements in obesity and glucose homeostasis. Irisin could be a protein therapeutic for human metabolic disease and other disorders that are improved with exercise.

PGC1 α (PPAR γ coactivator-1 α) is a transcriptional coactivator that mediates many biological programs related to energy metabolism. Originally described as a coactivator of PPAR γ that modulated expression of uncoupling protein 1 (UCP1) and thermogenesis in

Corresponding author: bruce_spiegelman@dfci.harvard.edu, Tel: 617-632-3567.

AUTHOR CONTRIBUTIONS

PB and BMS planned the majority of experiments and wrote the paper, while PB executed most of the experiments. JW performed a subset of cultured cell experiments and contributed valuable materials. MPJ and SPG performed the peptide fingerprinting identification of irisin cleavage. AK contributed with technical assistance and LY and SK performed the CLARK electrode experiments. EAB assisted with the hydrodynamic injections. JCL assisted with IV injections and KAR with bioinformatics. JZL and JHC performed *in vitro* experiments. PB and HT and LakePharma designed and provided FC-fusion proteins. KH and BFV performed the human cohort study, and MCZ and SC performed the electron microscopy studies.

Reprints and permissions information is available at www.nature.com/reprints.

The authors have no financial interest to disclose.

Supplementary Information is linked to the online version of the paper at www.nature.com/nature

brown fat¹, it has also been shown to control mitochondrial biogenesis and oxidative metabolism in many cell types. PGC1 α is induced in muscle by exercise and stimulates many of the best known beneficial effects of exercise in muscle: mitochondrial biogenesis, angiogenesis and fiber-type switching². It also provides resistance to muscular dystrophy and denervation-linked muscular atrophy³. The healthful benefits of elevated muscle expression of PGC1 α may go beyond the muscle tissue itself. Transgenic mice with mildly elevated muscle PGC1 α are resistance to age-related obesity and diabetes and have a prolonged life-span⁴. This strongly suggests that PGC1 α might stimulate the secretion of factors from skeletal muscle that affects the function of other tissues. In this paper, we show that PGC1 α stimulates the expression of several muscle gene-products that are potentially secreted, including Fndc5. The Fndc5 gene encodes a type I membrane protein that is processed proteolytically to form a new hormone secreted into blood, termed irisin. Irisin is induced in exercise and activates profound changes in the subcutaneous adipose tissue, stimulating browning and UCP1 expression. Importantly, this causes a significant increase in total body energy expenditure and resistance to obesity-linked insulin-resistance. Thus, irisin action recapitulates some of the most important benefits of exercise and muscle activity.

Transgenic PGC1 α in skeletal muscle induces browning of subcutaneous adipose tissue

Mice with transgenically increased PGC1 α in muscle are resistant to age-related obesity and diabetes⁴, suggesting that these animals have a fundamental alteration in systemic energy balance. We therefore analyzed the adipose tissue of the PGC1 α transgenic mice for expression of genes related to a thermogenic gene program and genes characteristic of brown fat development. There were no significant alterations in the expression of brown fat-selective genes in the interscapular brown adipose tissue or in the visceral (epididymal) white adipose tissue (Fig. 1a). However, the subcutaneous fat layer (inguinal), a white adipose tissue which is particularly prone to “browning” (i.e. formation of multilocular, UCP1 positive adipocytes), had significantly increased levels of UCP1 and Cidea mRNAs (Fig. 1b). We also observed increased UCP1 protein levels and more UCP1-positive stained multilocular cells in the transgenic mice, compared to controls (Fig. 1c and d). There are recent reports that exercise causes a mild increase in the expression of a thermogenic gene program in the visceral adipose tissue, a depot that has minimal expression of these genes⁵. Since it is the subcutaneous white adipose depot that has the greatest tendency to turn on a thermogenic gene program and alter the systemic energy balance of mice⁶, we re-investigated this with regard to browning of the white adipose tissues in two types of exercise. Similar to what has been reported⁵, a 2-fold increase in UCP1 mRNA expression was observed in the visceral, epididymal fat with three weeks of wheel running (Supplementary Fig. S1). However, a much larger change (approximately 25 fold) was seen in the same mice in the subcutaneous inguinal fat depot. Similarly, a small increase in UCP1 mRNA expression was seen in the epididymal fat with repeated bouts of swimming in warm (32°C) water (Supplementary Fig. S1); however a very large increase (65 fold) was observed in the inguinal white depot (Supplementary Fig. S1). Thus, muscle-specific expression of PGC1 α drives browning of subcutaneous white adipose tissue, possibly recapitulating part of the exercise program.

Conditioned media from PGC1 α -expressing myocytes induce browning of adipocytes in culture

The effect on browning of the adipose tissues from PGC1 α -expressing muscle could be due to either direct muscle-fat signaling or to another, indirect mechanism. To investigate this,

we treated cultured primary subcutaneous adipocytes with serum-free media conditioned by myocytes expressing PGC1 α or cells expressing GFP. As shown in Fig 1e, the media from cells expressing ectopic PGC1 α increased the mRNA levels of several brown fat-specific genes (Fig. 1e). This suggested that PGC1 α causes the muscle cells to secrete molecule(s) that can induce a thermogenic gene program in the cells.

Identification of candidate secreted proteins controlled by PGC1 α

We used a combination of Affymetrix-based gene expression arrays and an algorithm that predicts protein secretion to search for proteins that could mediate the browning of adipose tissues under the control of muscle PGC1 α (Methods). Proteins with mitochondrial targeting sequences were excluded, and all candidates were validated in gain-of-function systems for PGC1 α *in vivo* (Methods). Five proteins were identified as PGC1 α target genes in muscle and likely to be secreted: IL-15, Fndc5, VEGF β , Lrg1 and TIMP4 (Fig. 2a). Conversely, expression of these genes was reduced in mice with muscle-specific deletion of PGC1 α (Supplementary Fig. S2). Furthermore, they were also found to be increased at the mRNA level in muscle from exercised mice (Fig. 2b). The expression of this same set of genes was also examined in muscle biopsies from human subjects before and after a controlled period of endurance exercise⁷ (Fig. 2c). Fndc5, VEGF β and TIMP4 mRNAs were all significantly induced in humans with exercise. IL-15 has previously been reported as being secreted from muscle under the influence of exercise⁸, while the regulation of Fndc5, VEGF β , Lrg1 and TIMP4 by exercise has not been described. Fndc5 mRNA and brown fat markers in subcutaneous fat were not regulated by acute exercise, and Fndc5 mRNA was not induced by exposure to cold (4° C) for 6 hours (Supplementary Fig. S2).

Fndc5 robustly induces a brown fat gene program in cultured white adipose cells

Several of the proteins encoded by these genes were commercially available, so they were applied directly to primary subcutaneous white adipocytes during differentiation. Factors such as IL-15 or VEGF β had minimal effects on the expression of UCP1 and other brown fat genes at concentrations of 200 nM or higher. However, Fndc5 promoted a 7-fold induction of UCP1 mRNA at a concentration of 20 nM (Fig. 2d). The transcriptional changes induced by Fndc5 were addressed on a global scale using gene expression arrays (Supplementary Fig. S3). Strikingly, UCP1 and 3 other known brown fat genes, Elovl3, Cox7a and Otop1, were among the 8 most up-regulated genes (Supplementary Fig. S4). Conversely, genes characteristic of white fat development were down-regulated, such as leptin (Supplementary Fig. S3). These data strongly suggest that the activation of browning and thermogenic genes by Fndc5 is a major part of the action of this polypeptide on these cells.

The effects of Fndc5 treatment were remarkably robust; UCP1 mRNA was increased 7–500 fold in more than 10 experiment using Fndc5 at a concentration of 20 nM (Fig. 3a and Supplementary Fig. S5). Moreover, we could demonstrate a clear dose-dependence, with an effective range between 20 and 200 ng/ml (1.5 to 15 nM) (Fig. 3b). In contrast, BMP-7, reported as a potent inducer of browning⁹, had a much smaller effect (maximal of 2-fold) on the same cells at 3.3 μ M (Fig. 3a).

We also utilized immunohistochemistry to study cells treated with Fndc5 and observed a robust increase in UCP1-positive adipocytes with multilocular lipid droplets (Supplementary Fig. S4). Electron microscopic analysis of Fndc5-treated cells showed a higher density of mitochondria compared to control cells, consistent with a brown fat-like phenotype and elevated mitochondrial gene expression (Supplementary Fig S5). The sizes of mitochondria,

however, were similar between groups (Supplementary Fig. S4). Lastly, measurements of oxygen consumption provided functional evidence of increased energy expenditure with Fndc5 exposure. Total oxygen consumption was greatly increased (100%) by 20 nM of Fndc5, and the majority of this respiration was uncoupled (Fig. 3c). Thus, Fndc5 potently induces thermogenesis and a brown fat-like gene program in cultured adipocytes. In striking contrast, Fndc5 showed little or no effects on the classical brown fat cells isolated from the interscapular depot (Supplementary Figure S4).

We sought to define the time-frame during the differentiation process when Fndc5 was effective. Fndc5 was applied to cells in 2 day windows from day 0–6, and this was compared to cells where the protein was added during the entire 6 day differentiation process. As shown in Supplementary Figure S5, treatment during days 3–4 and 5–6 was effective at inducing UCP1 mRNA, though not as effective as when the Fndc5 was present throughout the differentiation process. Furthermore, treatment during the initial two days had no effect on UCP1 levels, suggesting that Fndc5 act mainly during the differentiation process of cells committed to the adipocytes lineage. Cyclic AMP (cAMP) is an important signaling pathway in thermogenesis, promoting the brown-fat gene program downstream of β -adrenergic stimulation. We therefore asked whether Fndc5 effects were additive or redundant with cAMP signaling. As shown in Fig. 3d, Fndc5-exposed cells increase UCP1 expression in an additive manner when exposed to forskolin, an adenyl cyclase activator. Two-way ANOVA tests demonstrated that there was a significant ($p < 0.01$) interaction between Fndc5 and forskolin treatment, indicating synergistic effects.

PPAR α acts downstream of Fndc5 to promote a thermogenic/brown fat program

A key question is how Fndc5 is able to stimulate a thermogenic gene program. One potentially important transcription factor induced by Fndc5, identified using gene expression arrays, was PPAR α . This nuclear receptor has been shown to drive UCP1 expression and several other genes involved in browning of adipose cells¹⁰. PPAR α is increased 3-fold at the mRNA level by Fndc5 treatment (Fig. 3e). Importantly, the Fndc5-mediated increase in UCP1 was significantly reduced when cells were simultaneously subjected to the selective PPAR α antagonist GW6471 (Fig. 3f). The functional interaction between the Fndc5 and GW6471 treatments on UCP1 expression was confirmed using two-way ANOVA ($p < 0.05$). Conversely, the PPAR α antagonist normalized the reduction seen in white adipose genes leptin and adiponectin after Fndc5-treatment. Together, these data suggest that Fndc5 acts to induce UCP1 gene expression, at least in part, via PPAR α .

Irisin is a cleaved and secreted fragment of Fndc5, found in mouse and human plasma

Fndc5 / Frcp2, also known as PeP, was previously shown to have a signal peptide, two fibronectin domains and one hydrophobic domain that is likely to be membrane-inserted^{11–12} (Fig. 4a). Previous studies did not investigate whether part of this protein might be secreted^{11–12}. With this structure in mind, we considered the possibility that Fndc5 might be synthesized as a type I membrane protein, followed by proteolytic cleavage, and release of the N-terminal part of the protein into the extracellular space. Thus, any C- or N-terminal tags would be lost during processing of the mature protein or interfere with localization. Indeed, expression of a C-terminally FLAG-tagged Fndc5 (Fig. 4a), did not result in any FLAG-immunoreactivity in the medium from cells expressing this construct (Fig. 4b). However, when we immunoblotted the same samples with an antibody that recognizes the endogenous Fndc5 protein, we could easily detect substantial amounts of

Fndc5 in the media at approximately 32 kD: this is slightly larger than the cellular Fndc5 (Fig. 4b). These data strongly suggests that Fndc5 is C-terminally cleaved, secreted and possibly further modified.

Western blot of media fractions with antibodies against wild-type Fndc5 showed multiple bands, suggestive of glycosylation, a common feature of secreted proteins. Treatment of supernatants from Fndc5-expressing cells with Peptide N-Glycosidase F (PNGase F) resulted in a significant size decrease as detected by SDS-gel electrophoresis, from 32 kD to 20 kD (Fig. 4c).

Mass spectrometry (MS) was used to determine the sequence of the Fndc5-derived polypeptide found in the media (methods). To do this, we fused the N-terminus of Fndc5 (without the signal peptide) to the C-terminus of the FC-domain of IgG. After purification and enzymatic deglycosylation of the secreted material, MS analyses indicated that secreted Fndc5 was truncated at glutamic acid 112 (not including the signal sequence), as shown in Figure 4e. The secreted portion of Fndc5 has remarkable conservation between species, with 100% identity between mice and humans (Supplementary Fig. S6). Since this distinct, secreted polypeptide has not been previously described and signals from muscle to other tissues (see above and below), we named it *irisin*, after **Iris**, the Greek messenger goddess.

The ability of the anti-Fndc5 antibodies to react with irisin allowed us to investigate the contribution made by irisin to the browning activity secreted by muscle cells expressing PGC1 α . Media conditioned by muscle cells that had forced expression of PGC1 α were incubated with control or anti-fndc5 antibodies before they were applied to the fat cell cultures. As shown in Supplementary Figure S6, the Fndc5 antibody caused a striking reduction in the ability of the PGC1 α conditioned media to induce UCP1 and Cidea mRNA in the primary inguinal cells. This suggests that irisin accounts for a significant fraction of this activity secreted by muscle cells with forced PGC1 α expression. We cannot, however, exclude the possibility that other factors might also contribute to this response.

Irisin is present in mouse and human plasma

We next analyzed levels of irisin in plasma from wild-type mice, using intravenous adenoviral delivery of full length Fndc5 as a positive control. This method results in strong forced expression from liver, and potential secretion to plasma, where we detected irisin using western blot after albumin/IgG-depletion and deglycosylation. As seen in Figure 5a, Fndc5-expressing virus resulted in a clear increase in an immunoreactive band at 22 kDa. Importantly, this was the only band altered on these blots. Using western blots of purified Fndc5 protein as a quantitative standard, irisin is present in the plasma of control mice at a concentration of approximately 40 nM. We also analyzed plasma of PGC1 α muscle-specific knockout mice as a negative control, and the irisin band at 22 kDa was decreased by 72% in these animals (Fig. 5b). Furthermore, an immunoreactive band of identical electrophoretic mobility was found in plasma from healthy human subjects (Fig. 5c). This band was greatly diminished when the anti-Fndc5 antibody was neutralized with an excess of antigen (Supplementary Fig. S7).

We examined blood levels of irisin after exercise in mice and human subjects. Mice had significantly elevated (65%) plasma concentrations of irisin after they were subjected to three weeks of free wheel running (Fig. 5d). Similar analyses in healthy adult humans subjected to supervised endurance exercise training for 10 weeks revealed a 2-fold increase in the circulating irisin levels compared to the non-exercised state (Fig. 5e). Thus, irisin is present in mouse and human plasma, and is increased with exercise. The increase in

circulating protein in both species is roughly proportional to the increases observed at the mRNA level in muscle (Fig. 2c).

Irisin reduces diet-induced obesity and insulin resistance *in vivo*

We used adenoviral vectors to express full-length Fndc5 (or a control GFP) and examined its biological and therapeutic effects. This method resulted in a 15-fold increase in liver Fndc5 mRNA, though the liver expresses very low endogenous levels of this mRNA. Plasma levels of irisin were increased 3–4 fold (Fig. 5a). The mice did not display any adverse reaction, and upon gross pathological examination, there was no apparent toxicity in any major organ system. There was also no increase in plasma AST levels, and inflammatory genes were not significantly altered in the liver when the two groups were compared (Supplementary Fig. S8). Ten days after injection, UCP1 mRNA was increased by 13-fold in the subcutaneous depot relative to the same depot in mice receiving the virus expressing GFP (Fig 6a,b); Cidea was also significantly up-regulated (Fig. 6a). There were no changes in expression of UCP1 in the interscapular BAT, but we did observe a minor elevation in PRDM16 and PGC1 α mRNA (Supplementary Fig. S8). The changes in gene expression in the subcutaneous adipose tissues were accompanied by a clear increase in the number of UCP1 positive, multilocular adipocytes (Fig. 6c). We did not, however, detect any change in body weight in the GFP vs. Fndc5 groups of animals. We observed similar results in young B/6 mice (Supplementary Fig. 9). Thus, moderate increases in circulating irisin can induce browning of white adipose tissues *in vivo*, including increased expression of UCP1.

Since activation of the classical brown fat or browning of white fat has been shown to improve obesity and glucose homeostasis *in vivo*^{6,13}, we delivered Fndc5-expressing adenovirus to mice rendered obese and insulin-resistance by feeding a high fat diet. We chose C57Bl/6 mice for these experiments because they are highly prone to diet-induced obesity and diabetes. The expression of irisin increased UCP1 gene expression to the same degree as in lean mice (Supplementary fig 9). There was also an elevation in expression of several mitochondrial genes (Supplementary Fig. S8). Notably, these changes occurred with only moderately increased irisin blood levels, 3-fold, compared to the GFP-expressing mice. This effect was accompanied with a large increase in oxygen consumption (Fig 6d), consistent with the gene expression data, and body weights of the irisin expressing mice were slightly reduced after 10 days compared to GFP-expressing controls (Fig. 6e). These effects of irisin on mitochondrial gene expression in the fat were not seen in skeletal muscle *in vivo* or in cultured myocytes (Supplementary Fig. S10). Irisin expression in the high-fat fed mice caused a significant improvement in glucose tolerance when compared to the control mice expressing GFP. In addition, fasting insulin was also reduced (Fig. 6f–g). These data illustrate that even moderately increased levels of circulating irisin potentially increases energy expenditure, reduces body weight and improves diet-induced insulin resistance.

Finally, we asked whether irisin is required for the exercise-induced effects on the subcutaneous white fat. Injection of anti-Fndc5 antibodies into mice prior to 10 days of swim training dramatically reduced the effect of this exercise on UCP1 and Cidea gene expression, compared injection of control antibodies (Fig. 6h). In contrast, PRDM16 mRNA levels were not increased with exercise and were also not affected by the anti-Fndc5 antibodies. Thus, irisin is required for a substantial part of the effect of exercise on these gene expression events in the browning of white fat.

DISCUSSION

Exercise has the capacity to improve metabolic status in obesity and type 2 diabetes via mechanisms that are poorly understood. Importantly, exercise increases whole body energy expenditure beyond the calories used in the actual work performed¹⁴. However, the relative contribution of the adipose tissues to this phenomenon has not been clarified. Since transgenic mice expressing PGC1 α selectively in muscle showed a remarkable resistance to age-related obesity and diabetes⁴, we sought factors secreted from muscle under control of this coactivator that might increase whole body energy expenditure. This paper describes a new polypeptide hormone, irisin, which is regulated by PGC1 α , secreted from muscle into blood and activates thermogenic function in adipose tissues. Irisin is remarkable in several respects. First, it has very powerful effects on the browning of certain white adipose tissues, both in culture and *in vivo*. Nanomolar levels of this protein increase UCP1 in cultures of primary white fat cells by 50 fold or more, resulting increased respiration. Perhaps more remarkable, viral delivery of irisin that causes only a moderate increase (~3 fold) in circulating levels stimulates a 10–20 fold increase in UCP1, increased energy expenditure and an improvement in glucose tolerance of high fat fed mice. Since this is in the range of increases seen with exercise in mouse and man, it is likely that irisin is responsible for at least some of the beneficial effects of exercise on the browning of adipose tissues and increases in energy expenditure. It is important to note that the evidence provided here does not exclude a role for other tissues besides muscle in the biological regulation and secretion of irisin.

Second, the cleaved and secreted portion of Fndc5, the hormone irisin, is highly conserved in all mammalian species sequenced. Mouse and human irisin are 100% identical, compared to 85% identity for insulin, 90% for glucagon and 83% identity for leptin. This certainly implies a highly conserved function that is likely to be mediated by a cell surface receptor. The identity of such a receptor is not yet known.

Based on the gene structure of Fndc5, with a signal peptide that was evidently missed in the studies of Ferrer-Martinez, et al, we considered that Fndc5 might be a secreted protein. Indeed, we have observed that the signal peptide is removed, and the mature protein is further proteolytically cleaved and glycosylated, to release the 112 aa polypeptide irisin. The cleavage and secretion of irisin is similar to the release/shedding of other transmembrane polypeptide hormones and hormone-like molecules such as the epidermal growth factor (EGF) and transforming growth factor alpha (TGF- α).

Since the conservation of calories would likely provide an overall survival advantage for mammals, it appears paradoxical that exercise would stimulate the secretion of a polypeptide hormone that increases thermogenesis and energy expenditure. One explanation for the increased irisin expression with exercise in mouse and man may have evolved as a consequence of muscle contraction during shivering. Muscle secretion of a hormone that activates adipose thermogenesis during this process might provide a broader, more robust defense against hypothermia.

The therapeutic potential of irisin is obvious. Exogenously administered irisin induces the browning of subcutaneous fat and thermogenesis, and it presumably could be prepared and delivered as an injectable polypeptide. Increased formation of brown or beige/brite fat has been shown to have anti-obesity, anti-diabetic effects in multiple murine models⁶, and adult humans have significant deposits of UCP1-positive brown fat¹⁵. Data presented here shows that even relatively short treatments of obese mice with irisin improves glucose homeostasis and causes a small weight loss. Whether longer treatments with irisin and/or higher doses would cause more weight loss remains to be determined. The worldwide, explosive increase

in obesity and diabetes strongly suggests exploring the clinical utility of irisin in these and related disorders.

Another potentially important aspect of this work relates to other beneficial effects of exercise, especially in some diseases for which no effective treatments exist. The clinical data linking exercise with health benefits in many other diseases suggests that irisin could also have significant effects in these disorders.

METHODS SUMMARY

Primary mouse stromal-vascular fractions from adipose tissues were differentiated as described⁶. Fndc5/irisin were purchased from ABNOVA (GST-fused), or produced from Syd Laboratories (GST-fused) or LakePharma (FC-fusions). Hydrodynamic injections were performed as described in Bell et. al,¹⁶. Electron microscopy was performed as described in Cinti et. al.¹⁷. Treadmill running was performed as in Wu et. al,¹⁸. Unless otherwise stated, bar graph data is presented as mean \pm SEM, and * $p < 0.05$ compared to control group. Students T-test was used for single comparisons and one-way ANOVA for multiple.

METHODS

Materials

Antibodies against UCP1, tubulin and Fndc5 were from Abcam. Forskolin, insulin, dexamethasone, rosiglitazone, GW6471 and antibody against flag were from Sigma. Primers for all qPCR experiments are listed in supplemental table I. Recombinant Fndc5, Lrg1, IL-15, VEGF β and TIMP4 were from ABNOVA (Taiwan). Coomassie staining kit and Lipofectamine 2000 was from Invitrogen.

Bioinformatic identification of PGC1 α -dependent signal-peptide proteins

All PGC1 α -induced genes as judged from gene expression analysis in MCK-PGC1 α muscle with a fold change of at least 2 and $p < 0.05$ were subjected to the following analysis. The protein sequence of the longest transcript were analyzed in the SignalP-software¹⁹ (<http://www.cbs.dtu.dk/services/SignalP/>). Sequences with positive S, C, Y and D-score were considered positive for a signal sequence. All positive proteins were then screened for mitochondrial target sequences (<http://www.cbs.dtu.dk/services/TargetP/>) whereas positive sequences were removed. All remaining hit proteins were then analyzed using qPCR in muscle from MCK-PGC1 α mice and myocytes over expressing PGC1 α .

Primary cell cultures and recombinant protein treatments

The SVF from inguinal fat depots of 8–12 week old BALB/C mice were prepared and differentiated for 6 days as described in²⁰. Rosiglitazone was used at the two first days of differentiation. For all experiments, unless otherwise indicated, recombinant Fndc5 was added to the culture media at a concentration of 1 μ g/ml the last 4 days of differentiation. Primary myoblasts were cultured and differentiated as described in²¹.

Preparation of protein fractions from cells and media

293HEK or primary myocytes were transfected by standard methods or transduced with adenovirus at a MOI of 20 as indicated. 24 hours after transfection, media was removed, and cells were washed in large volumes of PBS five times, followed by incubation in Freestyle serum-free media (GIBCO) for 24 hours. The cells and media were then collected separately, and media centrifuged $\times 3$ at 3000rpm to pellet debris. Thereafter, 1/4 volume of ice-cold TCA was added and precipitated protein was pelleted at 14000 rpm and washed $\times 3$ in acetone. Pellet was then dried and resuspended in SDS-containing lysis buffer. Protein

concentration was measured in both cell and media fraction and adjusted either by protein or volume as indicated.

RT-PCR

QPCR was carried out after Trizol-based RNA extraction using RNAeasy (Invitrogen) and thereafter SYBR green. All data was normalized to TBP, 18S or indicated in-house gene and quantitative measures obtained using the delta-delta-CT method.

Western blot and quantification

Protein amounts from all samples were assessed using the BCA-kit (Thermo Scientific) followed by protein concentration normalization prior to all western blot experiments. Western blot was carried out following standard procedure and final band intensity (QL-BG) was quantified using BioPix iQ²². All data was normalized to background and loading controls.

Additional methods

CLARK electrode measurements, energy expenditure in vivo, IGTT and immunohistochemistry against UCP1 were performed as described in⁶, with the exception that CLARK output was normalized to total cell protein. FC-fusion construction and protein purification was performed by LakePharma (Ca).

CLAM analysis of energy metabolism *in vivo*

C57/Bl6J mice were fed a high fat (60% Kcal) diet (D12492, Research Diets) for 20 weeks, starting at 6 weeks of age. Mice were then injected with indicated doses of adenovirus expressing GFP or Fndc5, and Comprehensive Lab Animal Monitoring Systems (CLAMS, Columbia instruments)-cage analysis was performed as described in Seale, 2011. Briefly, mice were acclimated in metabolic chambers for 2 days prior to analysis in order to minimize stress. CO₂ and O₂ levels were then collected every 36 minutes for a period of 3 days. Data on activity, heat generation and food intake were measured on more frequent intervals. Circadian rhythm was observed for most parameters Data was not normalized to body weights unless otherwise stated.

Mass spectrometry and peptide fingerprinting of purified, secreted Fndc5

Gel bands were digested with sequencing grade trypsin (Promega) or ASP-N(Sigma-Aldrich) as per manufactures' instructions. Extracted in-gel protein digests were resuspended in 8 µL 5% formic acid/5% acetonitrile, and 4 µL were analyzed by microcapillary liquid chromatography electrospray ionization tandem mass spectrometry (LC-MS/MS). Analyses were done on a LTQ Orbitrap Velos mass spectrometer (Thermo Fisher Scientific, Germany) equipped with a Thermo Fisher Scientific nanospray source, an Agilent 1100 Series binary HPLC pump, and a Famos autosampler. Peptides were separated on a 100 µm × 16 cm fused silica microcapillary column with an in-house made needle tip. The column was packed with MagicC18AQ C₁₈ reversed-phase resin (particle size, 5 µm; pore size, 200 Å; Michrom Bioresources). Separation was achieved through applying a 30 min gradient from 0 to 28% acetonitrile in 0.125% formic acid. The mass spectrometer was operated in a data dependent mode essentially as described previously²³ with a full MS scan acquired with the Orbitrap, followed by up to 10 LTQ MS/MS spectra on the most abundant ions detected in the MS scan. Mass spectrometer settings were: full MS (AGC, 1×10⁶; resolution, 6×10⁴; m/z range, 375–1500; maximum ion time, 1000 ms); MS/MS (AGC, 5×10³; maximum ion time, 120 ms; minimum signal threshold, 4×10³; isolation width, 2 Da; dynamic exclusion time setting, 30 sec). Following mass spectrometry data acquisition, RAW files were converted into mzXML format and processed using a suite of software

tools developed in-house for analysis. All precursors selected for MS/MS fragmentation were confirmed using algorithms to detect and correct errors in monoisotopic peak assignment and refine precursor ion mass measurements. All MS/MS spectra were then exported as individual DTA files and searched with no enzyme using the Sequest algorithm. These spectra were then searched against a database containing sequence of mouse Fndc5 in both forward and reversed orientations. The following parameters were selected to identify Fndc5: 10 ppm precursor mass tolerance, 0.8 Da product ion mass tolerance, fully tryptic or ASP-N digestion, and up to two missed cleavages. Variable modifications were set for methionine (+15.994915). In addition, a fixed modification for the carbamidomethylation for cysteine (+57.021464) was used as well. C-terminal fragment for Fndc5 was identified (KDEVTMKE) by trypsin digestion and reconfirmed by a separate ASP-N digestion.

Preparation of plasma samples for western blot

35 µl of mouse or human plasma was precleared for albumin/IgG using the ProteoExtract-kit (CalBiochem) as recommended by the manufacturer. Samples were then concentration to approximately 100µl and >8µg/µl, followed by deglycosylation of 150µg using PNGase F (New England Biolabs). Totally 80µl were then prepared containing 1X sample buffer with reducing agent and 1,7µg/µl protein, sonicated, boiled and analyzed using western blot against Fndc5 or indicated antibody.

Construction of the C- and N terminal FLAG fusion proteins (CTF and NTF) containing adenoviral constructs

The Fndc5 expression vector was purchased with a C-terminal FLAG-tag from OriGene. The QuickChange Multi Site XL Directed Mutagenesis Kit (Aligent Technologies) was used to introduce a FLAG tag downstream of the signal sequence and to mutate the c-terminal flag tag, thus resulting in the NTF-Fndc5 construct (Fig. 5a). The NTF and CTF Fndc5 constructs were then subcloned into the pENTR1a vector (Invitrogen) and recombined into the pAd-CMV-DEST-V5 vector (Invitrogen) and adenovirus was produced using the virapower system (Invitrogen), including three rounds of amplification. Thereafter, virus was concentrated using the Vivapure adenopack 100 (Sartorius Stedim Biotech) and buffer exchanges to saline reaching a concentration of 9–10 ifu/µl. A GFP-containing adenovirus previously used was prepared in parallel.

Transgenic mice

The MCK-PGC1α transgenic and muscle-specific PGC1α knockout mice have been described previously²⁴.

Exercise protocols

12 week old B6 mice were either exercised using swimming as described in²⁵, or using free wheel running as described in²⁶.

Human material and exercise training program

Blood samples and skeletal muscle biopsies were obtained from 8 male non-diabetic individuals before and after 10 weeks of aerobic training as described previously⁷. In brief, the exercise-training program consisted of cycling on stationary bikes with 4–5 sessions of 20–35 min per week at an average intensity of ~65% of maximal oxygen consumption. Informed consent was obtained from all volunteers before participation. The study was approved by the Local Ethics Committee and was performed in accordance with the Helsinki Declaration.

Supplementary Material

Refer to Web version on PubMed Central for supplementary material.

Acknowledgments

This study was supported by NIH grant DK54477, DK31405, DK61562 to BMS. PB and EAB were supported by the Wenner-Gren Foundation, Swedish Heart and Lung Foundation and SSMF. JW was supported by a postdoctoral fellowship from the American Heart Association (Founders Affiliate #09POST2010078). The animal procedures were in accordance with IAUC-protocols 110-2008 and 056-2009. The authors thank Drs. Susan Loffredo and Marc Kirschner for helpful discussions and suggestions on the manuscript.

References

1. Puigserver P, et al. A cold-inducible coactivator of nuclear receptors linked to adaptive thermogenesis. *Cell*. 1998; 92:829–839. [PubMed: 9529258]
2. Handschin C, Spiegelman BM. The role of exercise and PGC1alpha in inflammation and chronic disease. *Nature*. 2008; 454:463–469. [PubMed: 18650917]
3. Sandri M, et al. PGC-1alpha protects skeletal muscle from atrophy by suppressing FoxO3 action and atrophy-specific gene transcription. *Proc Natl Acad Sci U S A*. 2006; 103:16260–16265. [PubMed: 17053067]
4. Wenz T, Rossi SG, Rotundo RL, Spiegelman BM, Moraes CT. Increased muscle PGC-1alpha expression protects from sarcopenia and metabolic disease during aging. *Proc Natl Acad Sci U S A*. 2009; 106:20405–20410. [PubMed: 19918075]
5. Xu X, et al. Exercise ameliorates high-fat diet-induced metabolic and vascular dysfunction, and increases adipocyte progenitor cell population in brown adipose tissue. *Am J Physiol Regul Integr Comp Physiol*. 2011; 300:R1115–1125. [PubMed: 21368268]
6. Seale P, et al. Prdm16 determines the thermogenic program of subcutaneous white adipose tissue in mice. *J Clin Invest*. 2011; 121:96–105. [PubMed: 21123942]
7. Vind BF, et al. Impaired insulin-induced site-specific phosphorylation of TBC1 domain family, member 4 (TBC1D4) in skeletal muscle of type 2 diabetes patients is restored by endurance exercise-training. *Diabetologia*. 2011; 54:157–167. [PubMed: 20938636]
8. Nielsen AR, Pedersen BK. The biological roles of exercise-induced cytokines: IL-6, IL-8, and IL-15. *Appl Physiol Nutr Metab*. 2007; 32:833–839. [PubMed: 18059606]
9. Tseng YH, et al. Newrole of bone morphogenetic protein 7 in brown adipogenesis and energy expenditure. *Nature*. 2008; 454:1000–1004. [PubMed: 18719589]
10. Komatsu M, et al. Multiple roles of PPARalpha in brown adipose tissue under constitutive and cold conditions. *Genes Cells*. 2010; 15:91–100. [PubMed: 20002497]
11. Teufel A, Malik N, Mukhopadhyay M, Westphal H. Frp1 and Frp2, two novel fibronectin type III repeat containing genes. *Gene*. 2002; 297:79–83. [PubMed: 12384288]
12. Ferrer-Martinez A, Ruiz-Lozano P, Chien KR. Mouse PeP: a novel peroxisomal protein linked to myoblast differentiation and development. *Dev Dyn*. 2002; 224:154–167. [PubMed: 12112469]
13. Cederberg A, et al. FOXC2 is a winged helix gene that counteracts obesity, hypertriglyceridemia, and diet-induced insulin resistance. *Cell*. 2001; 106:563–573. [PubMed: 11551504]
14. Speakman JR, Selman C. Physical activity and resting metabolic rate. *Proc Nutr Soc*. 2003; 62:621–634. [PubMed: 14692598]
15. Enerback S. Human brown adipose tissue. *Cell Metab*. 2010; 11:248–252. [PubMed: 20374955]
16. Bell JB, Aronovich EL, Schreifels JM, Beadnell TC, Hackett PB. Duration of expression and activity of Sleeping Beauty transposase in mouse liver following hydrodynamic DNA delivery. *Mol Ther*. 2010; 18:1796–1802. [PubMed: 20628359]
17. Cinti S, Zingaretti MC, Cancelli R, Ceresi E, Ferrara P. Morphologic techniques for the study of brown adipose tissue and white adipose tissue. *Methods Mol Biol*. 2001; 155:21–51. [PubMed: 11293073]

18. Wu J, et al. The unfolded protein response mediates adaptation to exercise in skeletal muscle through a PGC-1alpha/ATF6alpha complex. *Cell Metab.* 2011; 13:160–169. [PubMed: 21284983]
19. Emanuelsson O, Brunak S, von Heijne G, Nielsen H. Locating proteins in the cell using TargetP, SignalP and related tools. *Nat Protoc.* 2007; 2:953–971. [PubMed: 17446895]
20. Kajimura S, et al. Initiation of myoblast to brown fat switch by a PRDM16-C/EBP-beta transcriptional complex. *Nature.* 2009; 460:1154–1158. [PubMed: 19641492]
21. Rasbach KA, et al. PGC-1alpha regulates a HIF2alpha-dependent switch in skeletal muscle fiber types. *Proc Natl Acad Sci U S A.* 2010; 107:21866–21871. [PubMed: 21106753]
22. Bostrom P, et al. The SNARE protein SNAP23 and the SNARE-interacting protein Munc18c in human skeletal muscle are implicated in insulin resistance/type 2 diabetes. *Diabetes.* 2010
23. Villen J, Gygi SP. The SCX/IMAC enrichment approach for global phosphorylation analysis by mass spectrometry. *Nat Protoc.* 2008; 3:1630–1638. [PubMed: 18833199]
24. Handschin C, et al. Skeletal muscle fiber-type switching, exercise intolerance, and myopathy in PGC-1alpha muscle-specific knock-out animals. *J Biol Chem.* 2007; 282:30014–30021. [PubMed: 17702743]
25. Bostrom P, et al. C/EBPbeta controls exercise-induced cardiac growth and protects against pathological cardiac remodeling. *Cell.* 2010; 143:1072–1083. [PubMed: 21183071]
26. Chinsomboon J, et al. The transcriptional coactivator PGC-1alpha mediates exercise-induced angiogenesis in skeletal muscle. *Proc Natl Acad Sci U S A.* 2009; 106:21401–21406. [PubMed: 19966219]

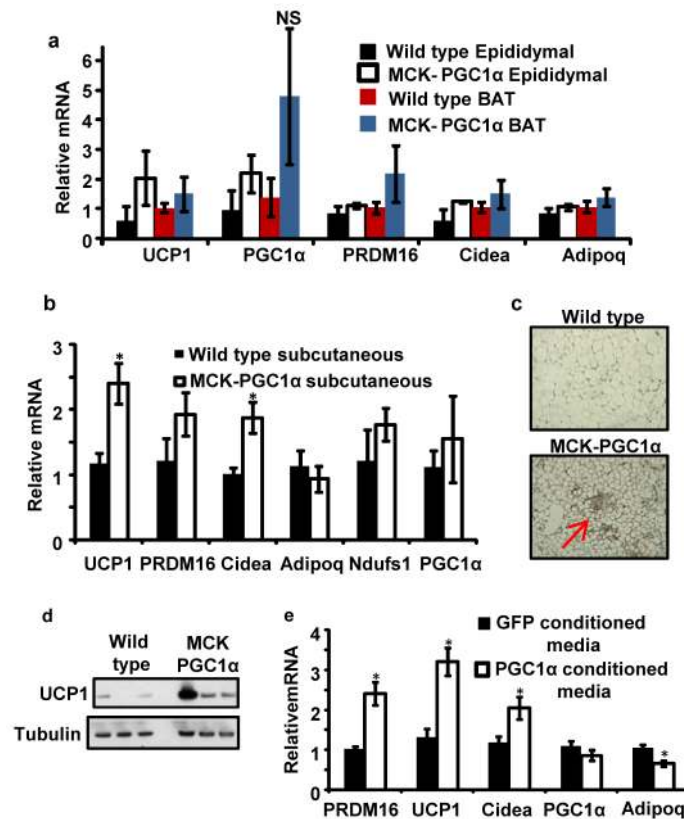


Figure 1. Muscle-specific PGC1 α transgenic mice have increased brown/beige fat cells in the subcutaneous depot

QPCR against brown fat and thermogenic genes in epididymal fat, classical brown fat (BAT) (a) and subcutaneous, inguinal (b) fat depots in MCK-PGC1 α transgenics or littermate controls. N=7 for each group, repeated in a separate cohort with similar results. c, representative immunohistochemistry against UCP1 in the inguinal depot from indicated mice. d, western blot against UCP1 in the inguinal fat depot (n=3 and repeated in an independent cohort with similar results). e, qPCR against indicated genes in adipocytes differentiated for 6 days from SVF cells. This was done in the presence of conditioned media from primary myocytes with forced expression of GFP or PGC1 α (representative for 3 independent experiments). Data is presented as mean \pm SEM, and * $p < 0.05$ compared to control group. Students T-test was used for single comparisons.

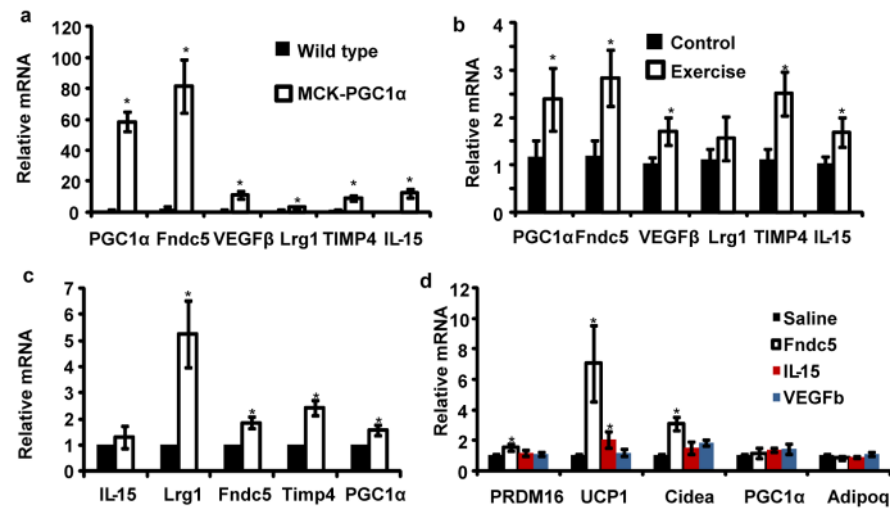


Figure 2. Fndc5 is induced with forced PGC1α expression or exercise, and turns on brown/beige fat gene expression

a, qPCR against indicated genes in skeletal muscle from MCK-PGC1α transgenic mice or littermate controls (n=7 from each group). **b**, qPCR against indicated genes in skeletal muscle from sedentary mice or mice given three weeks of free wheel running (n=10 from each group). Mice were rested for 12 hours prior to euthanization. **c**, mRNA expression levels from human muscle biopsies before and after 10 weeks of endurance exercise training (8 subjects included). All data points are normalized to baseline levels. **d**, SVF from the inguinal fat depot, differentiated into adipocytes for 6 days in the presence of saline or recombinant Fndc5 (20 nM), IL-15 (10μM) or VEGFβ (50μM). The graph show normalized mRNA levels of indicated genes. This experiment was repeated three times with similar results. For figure 2d, we performed one-way ANOVA tests where $p < 0.05$ for the effect of Fndc5 on UCP-1 and Cidea expression. All other statistics were performed using students T-test and bar graphs are mean \pm SEM.

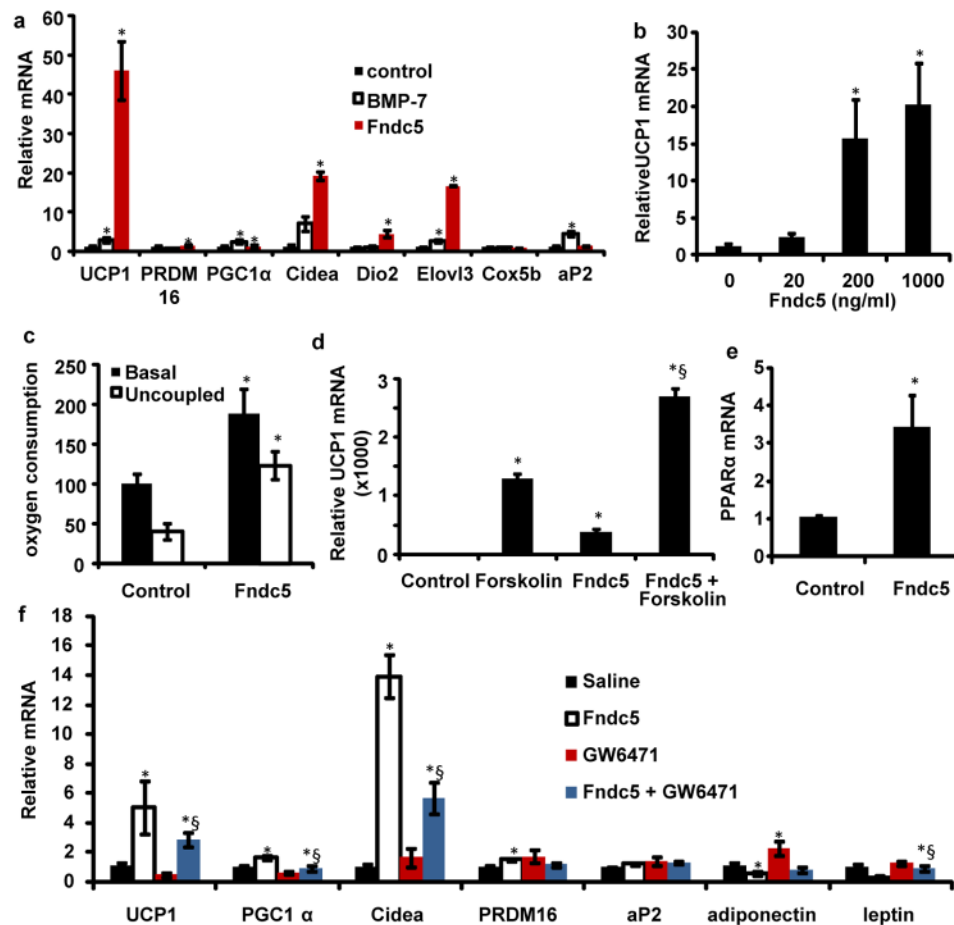


Figure 3. Fndc5 is a potent inducer of the brown/beige fat gene program

a, SVF from the inguinal fat depot was differentiated into adipocytes for 6 days in the presence of saline, recombinant Fndc5 (20 nM), or BMP-7 (3.3 μ M). The graph shows normalized mRNA levels for indicated genes. Similar results were obtained in more than 10 experiments with the fold induction of UCP1 between 7–500 fold. **b**, mRNA levels of UCP1 from inguinal-derived SVF treated with Fndc5 for 6 days at indicated doses. **c**, Clark electrode measurements of oxygen consumption in SVF from the inguinal fat depot, differentiated into adipocytes for 6 days in the presence of saline or recombinant Fndc5 (20 nM). Data is representative for three independent experiments and normalized to total cellular protein. **d**, qPCR of UCP1 mRNA from SVF, differentiated into adipocytes, and treated with Fndc5 or saline for 6 days followed by addition of forskolin for 8 hours. § indicates $p < 0.05$ compared to forskolin treatment. **e**, qPCR of PPAR α after 6 days of Fndc5 treatment (20 nM) during differentiation of primary SVF. **f**, SVF, differentiated into adipocytes, and treated with Fndc5 and/or GW6471 for 6 days. The graph shows qPCR of indicated genes, and § indicates $p < 0.05$ compared to Fndc5 treatment. For 3d and f; combined one and two-way ANOVA was used. All other statistics were performed using students T-test and bar graphs are mean \pm SEM.

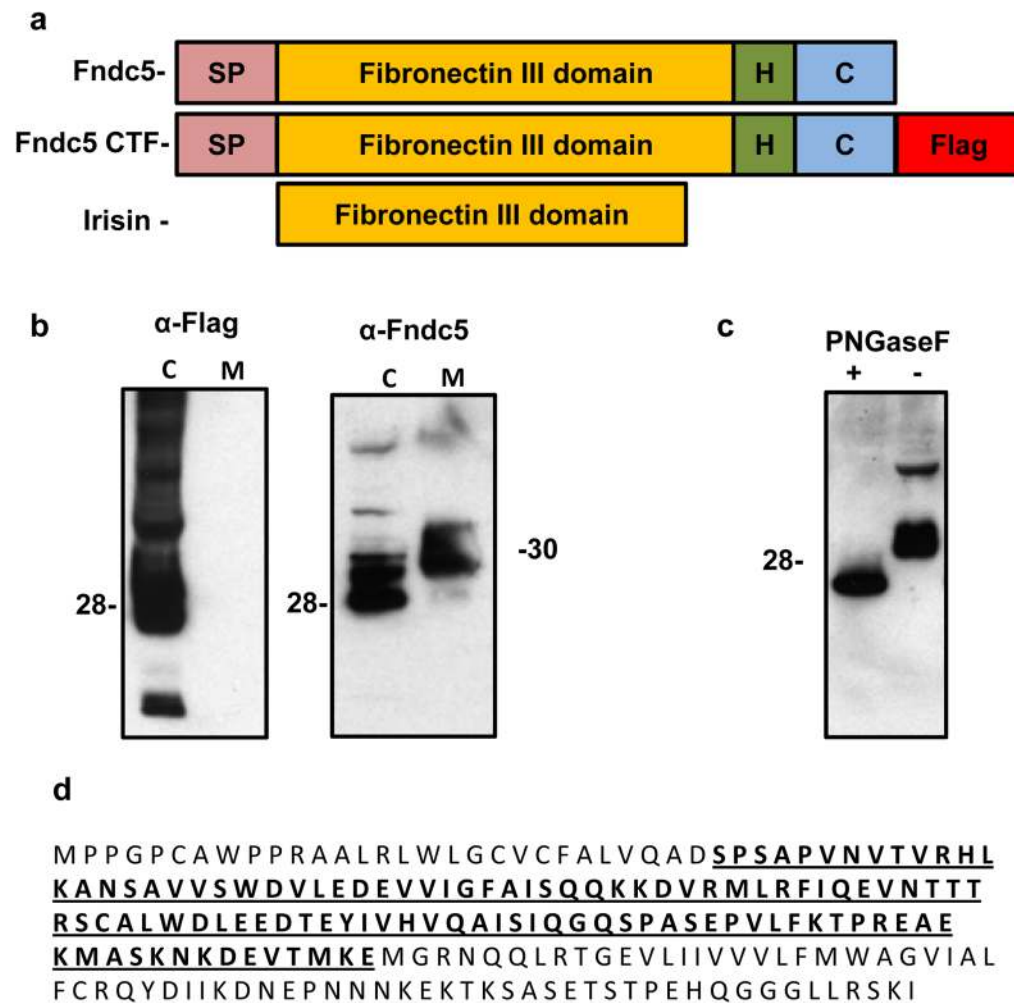


Figure 4. Fndc5 is proteolytically cleaved and secreted from cells

a, Schematic representation of the Fndc5 protein structure (top), flag-tagged Fndc5 protein (middle), and irisin (bottom). SP = signal peptide, H = hydrophobic domain, C = c-terminal domain, Flag = FLAG epitope. **b**, 293 cells transfected with a vector expressing the c-terminal flag tagged Fndc5 (CTF-F5, third panel from **a**), followed by isolation of cell and culture media protein. Samples were adjusted for protein content and western blots were performed against the FLAG antigen (left) or Fndc5 (right). This was repeated in several experiments with similar results. Adjusting for volume (instead of protein content) also gave similar results. C = cell fraction and M = media fraction. **c**, 293 cells transfected with a vector expressing Fndc5-CTF, followed by isolation of cell and media protein. Respective protein fraction was then treated with PNGase F followed by western blot against Fndc5 after SDS-PAGE. **d**, representation of the full-length Fndc5 and the irisin fragment mapped by mass spectrometry (bold and underlined).

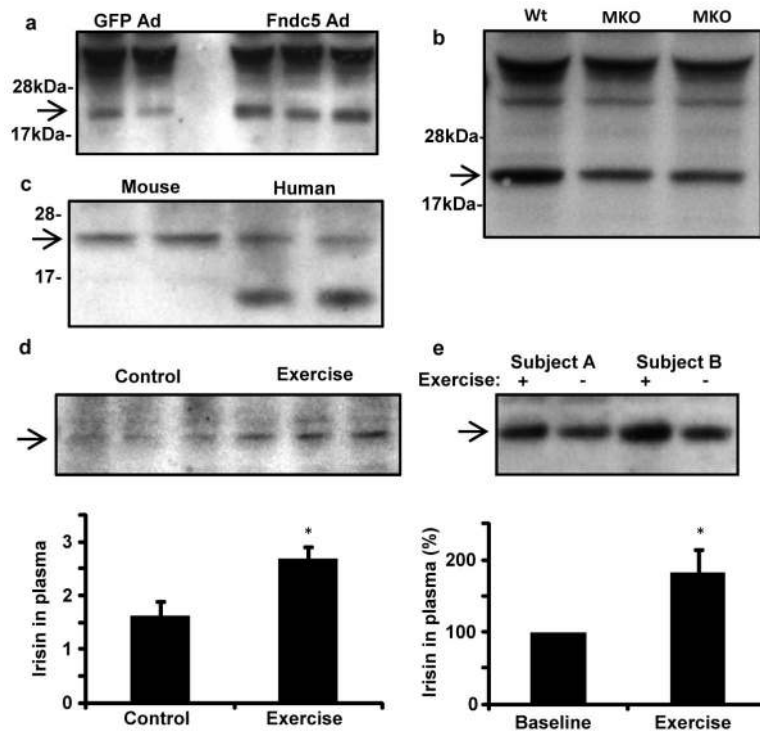


Figure 5. Detection of irisin in mouse and human plasma

a, Plasma from mice injected intravenously with adenoviral vectors expressing Fndc5 or GFP was subjected to western blot against Fndc5. **b**, western blot against irisin in plasma from muscle-specific PGC1 α knockout (MKO) mice or control littermates (flox/flox). **c**, western blot against irisin in plasma from wild-type mice or two healthy human subjects (representative for 8 subjects analyzed identically). **d**, western blot against irisin in serum from control or three weeks exercised mice, followed by 12h rest. Bottom panel shows quantification of the bands. **e**, western blot analysis of irisin in plasma from human subjects before and after 10 weeks of endurance exercise. 8 subjects in total were analyzed; quantification after internal normalization is displayed in bottom panel. For all plasma analyses, samples were depleted for albumin/IgG, and deglycosylated using PNGase F. Arrow indicated irisin band. Data is presented as mean \pm SEM, and * $p < 0.05$ compared to control group. Students T-test was used for single comparisons.

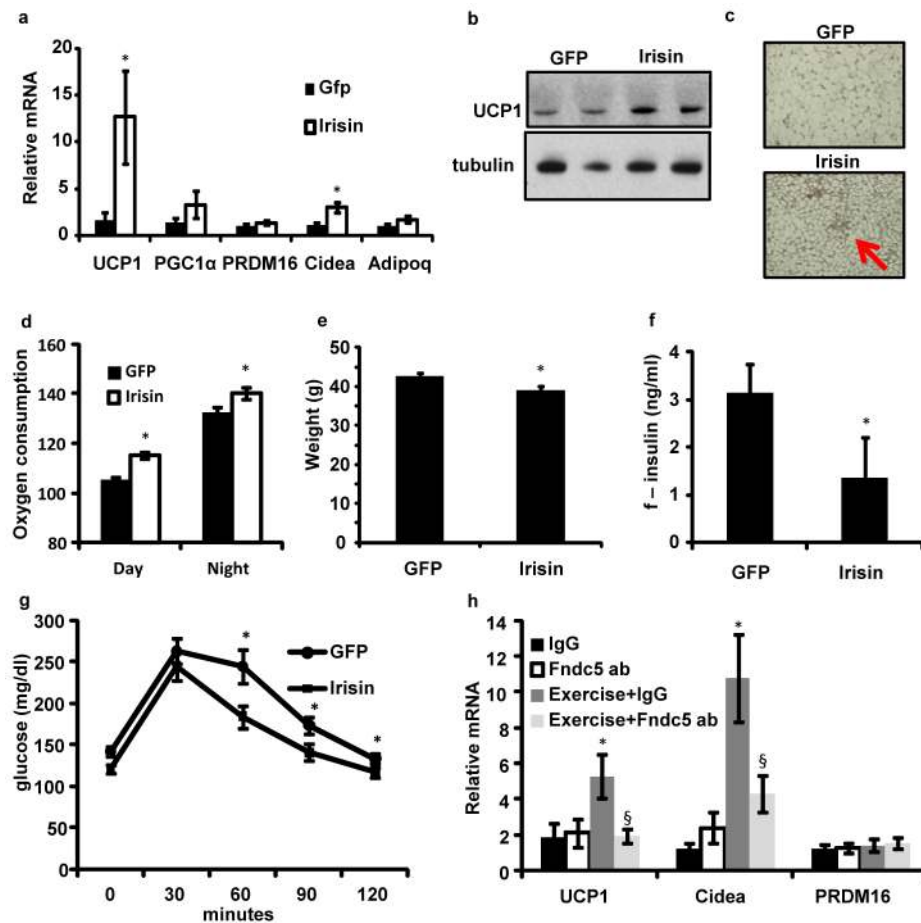


Figure 6. Irisin induces browning of white adipose tissues *in vivo* and protects against diet induced obesity and diabetes

a–c, Wild-type BALB/c mice were injected with 10^{10} GFP or Fndc5-expressing adenoviral particles intravenously ($n=7$ for each group). Animals were sacrificed after 10 days and inguinal/subcutaneous fat pads were collected and analyzed using qPCR analysis of indicated mRNAs (**a**) and western blot against UCP1 (**b**). **c**, representative images from immunohistochemistry against UCP1 in these mice. All results in **a–c** were repeated 2 times with similar results. **d–g**, C57/Bl6 mice fed a 60% kcal high fat diet for 20 weeks were intravenously injected with GFP or Fndc5-expressing adenovirus and all analyses were done 10 days thereafter ($n=7$ for both groups). **d**, oxygen consumption at day and night. **e**, body weights of 10 days after injection with indicated adenovirus in these mice. **f**, fasting plasma insulin measured using ELISA. **g**, intraperitoneal glucose tolerance test. **h**, mice were injected IP with 50 μ g of rabbit IgG or a rabbit anti-Fndc5 antibody and were either subjected to swimming for 7 days or kept sedentary ($n=10$ for all groups). Data displays mRNA expression levels from inguinal WAT. All data in **d–j** were performed at least twice in a separate mouse cohort with similar results. § $p<0.05$ compared to exercise + IgG. One-way ANOVA was used for statistics in **h**. All other statistics were performed using students T-test and bar graphs are mean \pm SEM.